

Dependence of TiO₂ Nanoparticle Preparation Methods and Annealing Temperature on the Efficiency of Dye-Sensitized Solar Cells

S. Nakade,[†] M. Matsuda,[‡] S. Kambe,[‡] Y. Saito,[‡] T. Kitamura,[‡] T. Sakata,[§] Y. Wada,[‡] H. Mori,[§] and S. Yanagida^{*‡}

Material and Life Science, Graduate School of Engineering, Osaka University, Suita, Osaka 565-0871, Japan, Research Center for Ultrahigh Voltage Electron Microscopy, Osaka University, Ibaraki, Osaka 567, Japan, and Nokia Research Center, Nokia-Japan Co., Ltd., 2-13-5, Nagata-cho, Chiyoda-ku, Tokyo 100-0014, Japan

Received: January 10, 2002; In Final Form: July 24, 2002

Performances of dye-sensitized solar cells prepared from nanoporous TiO₂ films with different TiO₂ nanoparticle preparation methods and different annealing temperatures are studied with various film thicknesses. The results show that the solar cells prepared at higher annealing temperatures have higher energy conversion efficiencies. Regarding film thickness, thin film electrode solar cells annealed at low-temperature show comparable efficiencies with those of the cells annealed at high temperature. The difference of the efficiency between the cells with the film annealed at different temperatures increases with the film thickness. To explain the observations, the surface area of the films, the amount of the adsorbed dye, and the diffusion coefficient and lifetime of electrons are measured. The amount of adsorbed dye per unit area is found to be independent of annealing temperature, while the diffusion coefficient and lifetime increase with the temperature. With trapping models, the measured increases of the diffusion coefficient with annealing temperature are interpreted with the change of the charge-trap density and neck growth between particles, which are suggested by transmission electron microscope and surface area measurements of the films. Diffusion lengths of electrons for each solar cell estimated from the diffusion coefficient and lifetime increase with annealing temperature. From the comparison between the short circuit currents of the solar cells with the diffusion lengths, it is concluded that the higher efficiencies of the solar cells prepared from high-temperature annealed films are attributed to their longer diffusion lengths of electrons.

Introduction

Dye-sensitized solar cells (DSC) have been attracting a lot of interests due to high energy conversion efficiency and the possibility of low production costs.¹ The solar cells consist of a dye adsorbed on a nanoporous film prepared from nanoparticles of metal oxide, typically TiO₂, and an electrolyte as a hole transport layer² containing redox couples. The dyes on the surface of the films absorb light and inject electrons into the conduction band of the metal oxide. To collect the electrons at a transparent conductive oxide (TCO) layer, the electrons should travel the distance in the conduction band from the point where the electrons injected to the TCO before recombination. Understanding the mechanism of the electron transport is one of the important aspects for further improvement of the solar cell efficiency.

The basic transport mechanism of electrons has been described with diffusion on the basis of the assumption of the absence of a large electric field gradient in the film.^{3–20} Diffusion coefficients of electrons in a nanoporous TiO₂ film have been reported by several groups. The measured values are much lower than those in a bulk crystal,^{7,9–11,17} and show light intensity dependence.^{4,9,17} The observations have been explained by models based on the electrons diffusing in the conduction

band having charge traps. In the model, the electrons spend a large fraction of their transit time at the intraband trap sites.^{5–9,13–20} The origin of trap sites has not been well-understood, but it has been assumed that they could be formed by titanium oxide amorphous layers, oxygen defects, boundaries between particles, and chemical surroundings.²¹ Particle synthesis method and annealing temperature are expected to change the trap site distribution and density, and consequently, affect the electron transport properties. However, these relationships and their effects on solar cell performance have not been studied in detail.

Currently nanoporous TiO₂ films for DSC are prepared mostly from nanoparticles followed by annealing typically at 450 °C in air. Lowering the temperature is one of the interests important to an industrial point of view. This is because it could reduce the fabrication cost and allow the use of plastic substrates.²² However, the performance of low-temperature annealed films has shown lower efficiency than that of high-temperature annealed films.^{22–26} To rationalize the lower efficiency, the diffusion coefficients of electrons in nanoporous films have been measured with different annealing temperatures. The results showed slower diffusion with lower annealing temperature,²⁵ which partially explained the lower efficiency. The decrease rate of the diffusion coefficients over the temperature difference was much larger than that for short circuit currents (J_{sc}) of solar cells. Such observations require more detailed studies. To explain the dependence of J_{sc} on annealing temperature, the charge collection efficiency was calculated using intensity

* To whom correspondence should be addressed. E-mail: yanagida@mls.eng.osaka-u.ac.jp.

[†] Nokia Research Center.

[‡] Material and Life Science.

[§] Research Center for Ultrahigh Voltage Electron Microscopy.

modulated photocurrent spectroscopy (IMPS) and intensity modulated photovoltage spectroscopy (IMVS).²⁶ However, the difference of calculated charge collection efficiency could not quantitatively explain the J_{sc} difference.

To study the dependence of TiO₂ nanoparticles and annealing temperatures on solar cell performance, three different types of TiO₂ nanoparticles are examined. Nanoporous films are fabricated from the particles with annealing at different temperatures. Dye-sensitized solar cells are made with the films having various thickness. The amount of the adsorbed dye is estimated for the DSC. The diffusion coefficient and lifetime of photogenerated electrons are measured and interpreted with trapping models. Short circuit currents of each solar cell are compared with diffusion lengths.

Experimental Section

Nanoporous films were prepared from colloidal suspension of TiO₂ nanoparticles dispersed in distilled water. Large size TiO₂ particles (Ishihara Sangyo, ST-41, 200 nm in diameter) were added (15 wt % of the small particles) on the colloidal suspension, except for the surface area measurements. The suspension was deposited on a transparent conducting glass (Nippon Sheet Glass, SnO₂:F, 8 ohm/sq) by using doctor blade technique. The films were annealed at 150 °C for 24 h or at a presented degree for 30 min in air. The thickness of the films was measured with a profiler (Sloan, Dektak3). The TiO₂ nanoparticles were synthesized with two different methods as described elsewhere.^{27,28} In short, one was prepared from hydrolysis of aqueous TiCl₄ solution, followed by autoclaving at 220 °C for 13 h. Another was prepared from hydrolysis of titanium tetraisopropoxide in the presence of nitric acid, followed by autoclaving at 220 °C for 12 h. In addition to these, one type of commercial nanoparticle (P25) was obtained from Nippon Aerogel. Crystallinity and crystalline size were measured with X-ray diffraction pattern with Cu K α radiation ($\lambda = 1.54$ Å) using an XRD Spectrometer (Rigaku RU-200B). A Rigaku Multiflex was used for in-situ XRD measurements. The porosity and surface area of the nanoporous films were measured with a nitrogen absorption apparatus (Quantachrome, Autosorb-1). Transmission electron microscopy was preformed by Hitachi H-9000, operating at 300 kV.

For photosensitization studies, the TiO₂ films were immersed in ethanol containing 0.3mM Ru-dye (Bu₄N)₂[Ru(Hdcbpy)₂(NCS)₂] (known as N719) for 12 h at room temperature. A counter electrode was prepared with platinum sputtering on a transparent conducting glass. The redox electrolyte consisted of 0.1 M LiI, 0.05 M I₂, 0.6 M 1,2-dimethyl-3-propylimidazolum iodide, and 0.5 M *tert*-butylpyridine in acetonitrile.

Photocurrent–voltage characteristics of solar cells were measured using a voltage-current source monitor (Advantest R6246) under AM1.5 simulated light source (Yamashita Denso, YSS-80). Solar cells were made by placing the Pt sputtered transparent conducting glass on the dyed TiO₂ film, and then the electrolyte was introduced from the edge of the two glass substrates just before the measurements.

The amount of adsorbed dye on the samples was estimated by measuring light absorption at 500 nm of the dye molecule ($\epsilon = 13300$ dm³ mol⁻¹ cm⁻¹) that was dissolved from the dye-adsorbed TiO₂ films into 0.1 M NaOH aq..

The diffusion coefficients (D) of electrons in the films were measured using pulsed laser induced photocurrent transient measurements. The measurements were performed without dye adsorption on the films in a two-electrode quartz cell.²⁹ The setup is described elsewhere.^{10,28} In short, a film was filled with

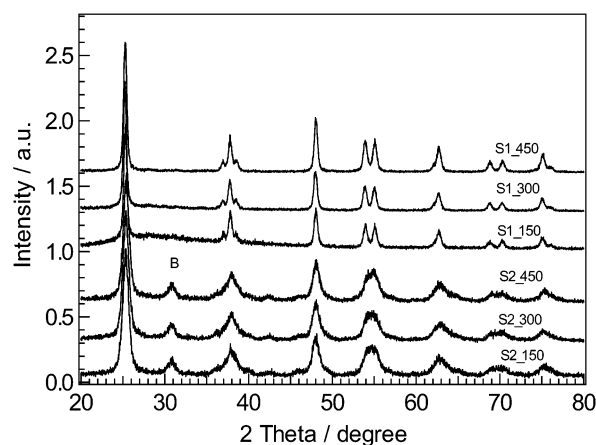


Figure 1. XRD pattern of nanoporous films prepared from TiO₂ nanoparticles with two different synthesis methods (sample denoted as S1 is from the hydrolysis of TiCl₄ and S2 is from the hydrolysis of titanium tetraisopropoxide). The films were annealed at 150 °C for 24 h, or 300 or 450 °C for 30 min in air. All peaks of S1 match with the reference data of anatase crystal, and S2 shows peaks corresponding anatase and brookite (denoted as B).

an electrolyte containing 0.7 M LiClO₄ in ethanol, which acts as a hole scavenger. A UV laser pulse (Quanta-Ray, Nd:YAG, 7 ns, $\lambda = 355$ nm) irradiated the film through the electrolyte. The current transients were recorded by a digital oscilloscope with different pulse energies. Mean electron densities in the film were estimated from the integration of the current transients. Measurements were repeated with different films, whose thicknesses were less than 10 μ m. Diffusion coefficients were estimated using measured current peak time (t) and film thickness (w) with a equation, $D = w^2/2t$. To estimate diffusion coefficients, it was assumed that the generated holes were filled during and just after the pulse irradiation, and the recombination of electrons was neglected during their transport for the range of sample thickness.^{28,30}

Electron lifetime in the solar cells at a open circuit condition was measured using intensity modulated photovoltage measurements (IMVS). The solar cells were irradiated by a diode laser (Coherent, LabLasers, $\lambda = 635$ nm) from the substrate side. A fraction of the laser intensity (9% of steady intensity) and modulation frequency were controlled with a function generator (Toho technical research, FG-02), and photovoltage responses were measured with a lock-in amplifier (Stanford Research Systems, SR810). Open circuit voltages and short-circuit currents under the diode laser irradiation without modulation were measured with a digital multi meter (Keithley 196 system DMM).

Results

Characterization of TiO₂ Films. Figure 1 shows XRD patterns of films prepared from hydrolysis of aqueous TiCl₄ solution (hereafter denoted as S1) and from hydrolysis of titanium tetraisopropoxide (hereafter denoted as S2) with different annealing temperatures (hereafter denoted as S1_150, meaning that the film was prepared from a colloidal suspension of S1 and annealed at 150 °C). All peaks from S1 showed good agreements with anatase reference data. The XRD pattern of S2 showed the mixture of anatase (80%) and brookite (20%). P25 consists of anatase and rutile (80:20, data not shown). Crystalline sizes of the films were estimated from the full width at half-maximum (fwhm) of the peak using Scherrer equation and the relative area of the diffraction peak at $2\theta = 25.4^\circ$. Both the fwhm and the relative area of the peak were not changed

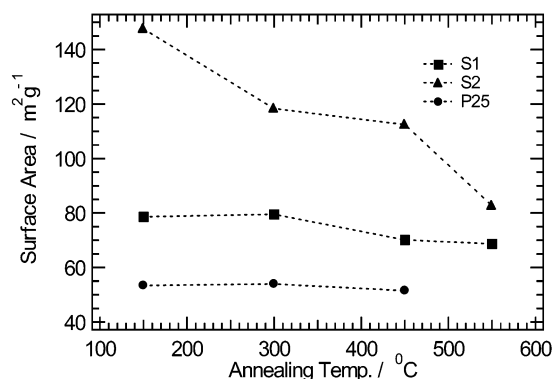


Figure 2. BET surface area of nanoporous TiO₂ films prepared from two different particles (S1 and S2), and films prepared from commercial TiO₂ particles (P25) at various annealing temperatures.

up to 450 °C for the all particles. The estimated sizes were 19 nm for S1, 12 nm for S2, and 21 nm for P25, regardless of the annealing temperature up to 450 °C. In situ XRD measurements of the three particles above 450 °C showed that the crystalline size of P25 did not change significantly up to 800 °C, while that of S1 and S2 started increasing above 600 and 450 °C, respectively (data not shown). The changes of crystalline size may be caused by sintering among particles and further crystallization. The use of lower starting temperature to increase the size for S1 and S2 suggests the ease of connecting these particles.

Figure 2 shows BET surface area of each films with various annealing temperatures. As the temperature was increased, the areas of S1 and S2 were decreased, while P25 showed a constant value. Since the crystalline size was not changed with annealing temperature up to 450 °C, the decrease of the surface area could be caused by neck growth between particles, but the lattice mismatch would occur at the boundaries. The large decrease of S2 could mean that the surface of the particle may be easier to deform with dehydration. To the contrary, the surface of P25 could be described as being hardened against temperature. The interpretation of the BET measurements seem to be consistent with the XRD analysis results of the crystalline size changes caused by the annealing at high temperature.

Figure 3 shows TEM images of the three different TiO₂ with two different annealing temperature. They showed the particles are made of single crystal with probably very thin amorphous layers of titanium oxide on the surface. Clear boundaries between particles also appeared in the films annealed at 450 °C, while few are found in the films annealed at 150 °C, based on visible inspection.

Characteristics of TiO₂ Films as Solar Cells. Figure 4 shows the energy conversion efficiency of N719 sensitized TiO₂ films with two different annealing temperatures and different film thickness. The measurements were repeated with several sets of films, and the data shown here were from the set, which showed the highest values. Table 1 summarizes the photocurrent–voltage characteristics with the porosity, surface area, and the amount of the adsorbed dye of the all samples. All the films annealed at 450 °C showed a higher efficiency than that annealed at 150 °C. For the thin films, the difference of the efficiency depending on the temperature was small. The efficiencies of the all the 450 °C annealed films increased with film thickness, while the efficiency of the 150 °C annealed films became maximized within 6 μm thickness.³¹ Taking into account of the measured surface area, the adsorbed dye per unit area differs within 10% in relation to the differences of film thicknesses and annealing temperatures. From the table, it can

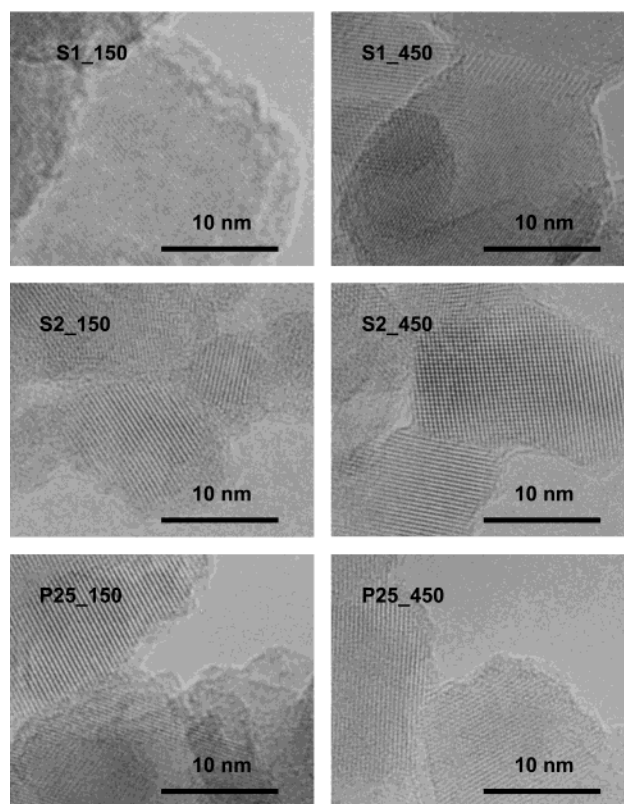


Figure 3. TEM micrographs of TiO₂ nanoporous films. The films were prepared from particles with different synthesis methods (S1, S2, and P25) and annealing temperatures (150 °C for 24 h or 450 °C for 30 min).

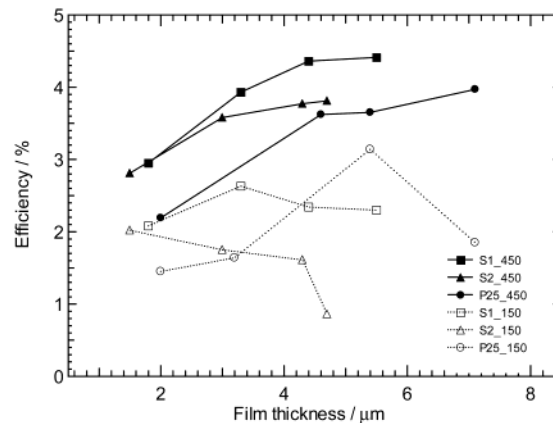


Figure 4. Energy conversion efficiency of Ru–dye (N719) sensitized TiO₂ films under AM1.5 simulated light (100mW/cm²) with different film thicknesses. The films are the same as used for the TEM measurements on Figure 3.

be seen that the lower efficiency of the lower annealed films is mainly due to their lower short circuit currents, which is not caused by the amount of adsorbed dye.

Diffusion Coefficients and Lifetime of Electrons. To estimate the diffusion length (L) of electrons in TiO₂ film, the diffusion coefficient and lifetime (τ) of electrons were measured. Figure 5 shows the diffusion coefficients of the films with different particles and annealing temperatures at 150 and 450 °C as a function of mean electron density. Among the same particles, the increase of annealing temperature resulted in the increase of the diffusion coefficient. Compared with different samples, S1 showed the largest values for both temperatures. Remarkably, D of S1_150 had faster D values than those of S2_450 and P25_450 at lower electron densities.

TABLE 1: Performance of Solar Cells with Nanoporous Film Characteristics^a

	J_{sc} mA cm ⁻²	V_{oc}/V	efficiency/%	porosity/%	surface/m ² g ⁻¹	dye/ 10 ⁻¹¹ mol/cm ²
S1_450	9.84	0.78	4.41	53	70	11
S1_150	4.95	0.77	2.63	53	79	12
S2_450	9.52	0.73	3.81	38	118	9.3
S2_150	4.04	0.72	2.02	38	148	8.4
P25_450	8.93	0.75	3.97	60	54	9.2
P25_150	5.89	0.77	3.14	62	54	9.8

^a The values for I - V characteristics are chosen to appear the highest values. The radiant power is 100 mW cm⁻².

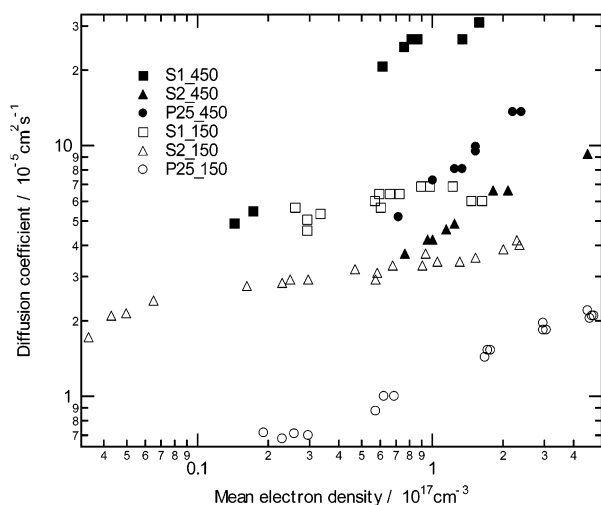


Figure 5. The electron diffusion coefficients of the TiO₂ films filled with 0.7 M LiClO₄ in ethanol as a function of mean electron density in the films. The films are the same as those used for Figures 3 and 4. These measurements of D were performed without the dye adsorption.

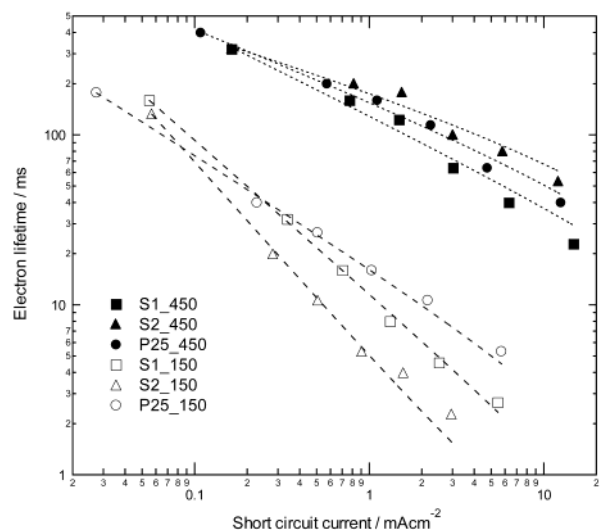


Figure 6. Dependence of electron lifetime of dye-sensitized solar cells, which are the same as measured on Figure 4, on short circuit current. The J_{sc} was proportional to the incident light intensities for all samples.

IMVS measurements were performed on the solar cells fabricated with the three different TiO₂ particles and different annealing temperatures. The voltage responses to modulation frequency showed a semicircle on a plot of $\text{Re}(\Delta V_{oc})$ vs $\text{Im}(\Delta V_{oc})$, which was similar with reported results, and thus, the lifetime was derived from the frequency at the minimum of the semicircle (ω_{min}) of the IMVS responses.^{9,15} Figure 6 shows the lifetime of the all samples as a function of J_{sc} of the cells. Note that the J_{sc} was proportional to the light intensities for the light intensity range used here for all samples. The results showed that the increase of annealing temperature resulted in longer electron lifetimes for the all particles.

TABLE 2: Characteristic Slopes of the Plots of D and τ for Various Nanoporous TiO₂ Films

	the slope of D	the slope of τ
S1_450	0.5	0.45
S1_150	0.05	0.9
S2_450	0.2	0.25
S2_150	0.1	1.1
P25_450	0.5	0.45
P25_150	0.55	0.6

TABLE 3: Comparison between Diffusion Length and Short Circuit Current^a

	$D/10^{-5}$ cm ² s ⁻¹	τ /ms	L/μ m	J_{sc} /mA cm ⁻²
S1_450	45	30	37	9.84
S1_150	6	3	4.2	4.95
S2_450	6	60	19	9.52
S2_150	3.2	1.5	2.2	4.04
P25_450	12	45	23	8.93
P25_150	1.1	7	2.8	5.89

^a The values of D and τ are estimated from Figure 5. and 6, respectively. The values are chosen at the electron density of 1×10^{17} cm⁻³ and τ at 4.5 mA/cm², for 150 °C annealed films, and 2×10^{17} cm⁻³ and τ at 9 mA/cm², for 450 °C annealed films to represent the similar condition under one sun irradiation. The J_{sc} values of the solar cells are the highest observed values.

The slopes of the double logarithmic plot of D and τ have been reported by several groups. Here we also obtained the slopes for all samples, and listed in Table 2. The slopes from higher temperature annealed films showed the comparable values with that reported by others,^{9,15-18} while not all of the slopes from low-temperature annealed films do not.

Current–Voltage Characteristics and Diffusion Length.

Table 3 shows D at the electron density (n) of 1×10^{17} cm⁻³, and τ at 4.5 mA cm⁻² for 150 °C annealed films, and D at the n of 2×10^{17} cm⁻³, and τ at 9 mA cm⁻² for 450 °C annealed films, diffusion length obtained by $\sqrt{D\tau}$ and J_{sc} for the all films. Here, the estimated L does not represent the L under the short circuit condition. This is because the lifetime of electrons depends on the solar cell operating voltage, and the lifetime at short circuit has been reported to be longer than that at open circuit condition.³² However, the estimated L here should represent the film property and are convenient to compare the each films. The values of D and τ were chosen at close to the condition under one sun irradiation, and the obtained L was comparable with the previous report.⁹ The diffusion lengths of the all 150 °C annealed films were less than one-fifth of those of high-temperature films, even for S1_150 which showed faster D . For the 450 °C annealed films, the diffusion lengths are longer than the thickest films used here. This explains the increase of J_{sc} with film thickness. Due to the shorter diffusion length of the low-temperature annealed films, J_{sc} saturated at thin thickness of the film, resulting in lower J_{sc} .

Discussion

The above results showed the diffusion lengths of electrons in TiO₂ film affected strongly on the short circuit currents of

the solar cells. The diffusion lengths were influenced by the TiO₂ nanoparticle synthesis methods and film annealing temperatures. To design electrode for the solar cells, it is important to understand how these could influence the diffusion coefficients and lifetime of electrons, as well as other facts affecting short circuit currents.

Diffusion Coefficients of Electrons. Electron diffusion in nanoporous films filled with an electrolyte could be interpreted with ambipolar diffusion mechanism.^{17,30,33} This means the measured diffusion coefficient should be interpreted with the density and diffusion coefficient of cations in the electrolyte. However, since ambipolar diffusion coefficient is determined by minority carriers, which are electrons for our experimental conditions, the values in Figure 4 should represent the diffusion coefficients of electrons in the films. In a previous report, the influences of cations on the diffusion coefficients were studied.³³ The results showed that diffusion coefficients depended on the concentration of cations rather than the species of cations, while the amount of photogenerated charges depended highly on the species. Hence, the diffusion coefficients measured here without dye could be assumed that in the solar cell configuration, and this probably explains the comparable L estimated here with previous reports.⁹

On the bases of trapping models, the measured diffusion coefficients are interpreted as effective diffusion coefficients, since electrons are assumed to stay at trap sites for most of their transit time. The effective diffusion coefficients may be expressed with the diffusion coefficient of electrons without traps D_{free} as $D_{\text{eff}} \approx D_{\text{free}}(dn_{\text{cb}}/dn)$, where n_{cb} is the density of electrons on the conduction band and n is the total density of electrons in the film.¹⁵ Thus, the energy distribution of the trap sites and light intensity affect the D_{eff} . The distribution of the traps may be expressed with an exponential function with a characteristic slope α by

$$N(E) = N_{\text{tot}} \frac{\alpha}{kT} e^{\alpha(E - E_c)/kT} \quad (1)$$

where k is Boltzmann's constant, N_{tot} is the total density of states, E_c is the energy of the conduction band edge, and T is temperature. The observed relationship of D and light intensity (I) is a power law,^{9,17,19} and this could be expressed with the slope¹⁹ as

$$D_{\text{eff}} \propto I^{1-\alpha} \quad (2)$$

The relationship between N_{tot} and D_{eff} could be described as¹⁹

$$D_{\text{eff}} \propto N_{\text{tot}}^{-2/3} \quad (3)$$

Since the nanoporous films contains a lot of boundaries between particles, the D_{free} would be the sum of the diffusion coefficients of the conduction band and the rate to jump across the boundary. The diffusion coefficients of the films annealed at 450 °C in Figure 5 were higher than those of low-temperature annealed films, compared among the same type of TiO₂ particles. These changes could be caused by the decrease of trap density and/or neck growth between particles with by annealing.

For P25, D of P25 450 was increased more than 6 times as that of P25_150. To explain the difference in terms of the trap density, N_{tot} should be decreased by more than a factor of 10, according to eq 3. The trap density of TiO₂ nanoporous films

annealed at 450 °C could be in the order of 10^{17}cm^{-3} .^{5,19} The difference of the traps to account for the observed D seems relatively large if it were assumed that the all traps were located at boundaries between the particles and removed by the annealing at 450 °C.³⁴ Hence, the difference of D of P25 may be more likely to be associated with the difference of the electron hopping rate between the particles, which depend on the degree of the neck growth between particles. The rate of the move across the boundaries may be treated with the degree of electron scattering caused by the lattice mismatch at the boundaries and distance between particles; see Figure 3.

The hypothesis mentioned above seems to be also supported with the observations of the surface area decrease of films with increasing temperature, i.e., the surface area decrease may be caused by the increase of the neck cross section between particles. The surface area decrease also indicates that the partial crystallization could occur at 450 °C. For S1 and S2, the measured diffusion coefficients may be postulated with the sum of neck growth and the decrease of trap density. For boundaries between particles, particles, whose surface is easy to deform and connect to other particles, give higher diffusion coefficient at the boundaries, and consequently increase the diffusion coefficient of the nanoporous film. Among the films annealed at 150 °C, D of S1_150 and S2_150 are higher than that of P25 150. These facts agree with the interpretation of change of the surface area, and S1 and S2 are easy to connect at even low temperature. The clear boundaries for S1_450 and S2_450 in Figure 3 imply also the decrease of traps at the boundaries and probably on the surface. For P25, it seems to have more difficulty to form connection between particles at the low annealing temperature, resulting less electrical conductivity of the film. Between the annealing temperature difference, S1 and S2 showed less increase rates of D against the annealing temperature than that of P25. For S1, and S2, we could not rule out if the decrease of trap density contribute more on the increase of D .

Other possible parameters affecting D are crystallinity and particle sizes. If particle boundaries caused less D , the mixture of crystallinity also could cause less D , which might explain the lower D of S2_450 and P25 450 than that of S1_450. Between S2 and P25, the particle size of S2 is smaller than that of P25. If the traps were located on the surface with similar density, a larger particle size with less surface area would provide faster transport rate. The difference of the size would change the number of boundaries, which also could change the diffusion coefficient. However, these hypothesis are preliminary and need to be substantiated further.

Based on the observations, to increase D , it seems better to have particles of single crystallinity and easiness to form neck between particles. This seems to explain the highest D of S1_450. D of S1_150 was faster than that of S2_450 and P25_450 at lower electron density. This clearly shows that the diffusion coefficients depend on the surface conditions as well as annealing temperature.

Electron Lifetime in Nanoporous Films. It has been reported that the electron lifetime in DSC is in millisecond to second order, and is related to the inverse power of the light intensity.^{9,15,16,20} The experimental results of the electron lifetime have been studied with two different models. The relationship between lifetime and light intensity can be expressed from trapping models as

$$\tau \propto I^{-\beta} \quad (4)$$

where I is light intensity and β is a slope,²⁰ or as

$$\tau = \frac{1}{2kn} \quad (5)$$

where k is a constant and n is the small perturbation of electron density, based on the second-order reaction with I^-/I_3^- redox couples.^{9,35} Equation 5 is equivalent with $\tau = I^{-1/2}$, in terms of the incident light intensity.

Among the films annealed at 450 °C, the films having faster D showed shorter lifetimes. This could be interpreted with trapping models, which assume the shorter time interval between hops increases the chance to encounter holes, that are I_3^- in an electrolyte and dye cations for the solar cells, resulting in shorter lifetimes.¹⁸ On the other hand, as is seen, the lifetime of higher temperature annealed films showed longer lifetime than that of low temperature.³⁶ The recombination path in DSC would be both from the conduction band and surface trap sites. If the dominance of recombination were via trap sites, the same mechanism as for the increase of diffusion coefficients due to the decrease of trap sites could be postulated to account for the increase of lifetime with annealing temperature.

Park et al. reported that the electron lifetime increased with annealing temperature,²⁶ which is consistent with our results. Note that however our results indicated that the change of lifetime did not affect the photovoltage as much as that reported in ref 26.

Short Circuit Currents. The measured diffusion coefficients here are interpreted as diffusion of thermalized electrons, which assumes that electrons interact with all traps. However, it has been pointed out that some electrons are collected before enough interactions occur with traps, when a solar cell is irradiated from the TCO/substrate side.¹⁹ With applying the idea to our measurements, the diffusion coefficients measured from the films having more than a few micron thickness are lower than the actual values for the electrons close to TCO under solar cell operation. In addition to this, the gradient of Fermi level,¹⁹ and/or electric potential difference could exist in the films, mostly at the interface of the TCO/TiO₂.³⁷ Hence the electrons close to the interface may not be explained adequately only with diffusion. However, the observations of the decrease of J_{sc} with the increase of film thickness for low-temperature annealed films could be interpreted in reference to their lower diffusion lengths. This result supports the assumption that the electric field is effectively constant for most range of the film. On the other hand, the longest L of S1_150 could not supply the highest J_{sc} , among the 150 °C annealed films, which needs further explanations.

Another possible contribution to J_{sc} is a charge injection efficiency from dye to TiO₂ particles, which could depend on the adsorption properties relating with the surface conditions of TiO₂.³⁸ One might expect that the difference of the properties could depend on the annealing temperature.²⁶ In our previous paper, to examine the effect of the surface conditions on electron diffusion coefficient, we annealed P25 TiO₂ particles at 450 °C before the preparation of colloidal suspension, and the diffusion coefficients of films prepared from the particles showed the same as that prepared without the annealing.²⁵ This implies that the surface conditions of P25 did not change significantly by the annealing. Hence, the adsorption condition of the particles may also not be affected by the annealing temperature. The thinnest film of P25_150 seems to have enough diffusion length and adequate dye adsorption properties. Hence, the measured low J_{sc} of P25_150 compared with P25_450 seems to be explained also by other reasons.

This argument of dye adsorption might not be true for S1_150 and S2_150, since they have not experienced 450 °C atmosphere before the annealing to prepare the films and the surface condition may differ between the temperatures. For these films, it may be necessary to reconsider the estimated values of the adsorbed dye per unit area with the particle surface condition dependent charge injection efficiency. This issue requires further investigation and the work is in progress.

Conclusions

Dye-sensitized solar cells were prepared from TiO₂ nanoparticles synthesized by three different methods. The thickness and annealing temperature of TiO₂ electrodes for the solar cells were varied. It was found that the energy conversion efficiencies of the solar cells prepared from 150 °C annealed films were lower than those of the 450 °C annealed films, regardless of the TiO₂ synthesis methods. The lower efficiencies of the 150 °C annealed films were not due to their lower open circuit voltage but lower short circuit current. The amount of adsorbed dye per unit area could not explain the difference of J_{sc} , indicating the possibility of the surface condition dependence of charge injection efficiency. The electron diffusion lengths were estimated from the diffusion coefficients and lifetimes for the all TiO₂ electrodes. The diffusion lengths of the all 150 °C annealed films were much lower than that of 450 °C annealed films. The difference of diffusion lengths were interpreted with TEM, XRD, and BET surface area measurements, and the longer diffusion lengths of high-temperature annealed films were attributed to the neck growth between particles and the changes of charge trap density. These facts agree with the maximization of the energy conversion efficiency appeared at the thinner thickness of the electrodes annealed at the 150 °C, compared with that of the 450 °C annealed samples.

Acknowledgment. This work was partially supported by Grant-in-Aid for Scientific Research (A) (No. 11358006), and by Grant-in-Aid for the Development of Innovative Technology (No. 12310) from the Ministry of Education, Culture, Sports, Science and Technology of Japan.

References and Notes

- O'Regan, B.; Grätzel, M. *Nature* **1991**, 353, 737.
- Kubo, W.; Murakoshi, K.; Kitamura, T.; Yoshida, S.; Haruki, M.; Hanabusa, K.; Shirai, H.; Wada, Y.; Yanagida, S. *J. Phys. Chem. B* **2001**, 105, 12809.
- Södergren, S.; Hagfeldt, A.; Olsson, J.; Lindquist, S.-E. *J. Phys. Chem. B* **1994**, 98, 5552.
- Cao, F.; Oskam, G.; Meyer, G. J.; Searson, P. C. *J. Phys. Chem. B* **1996**, 100, 17021.
- de Jongh, P. E.; Vanmaekelbergh, D. *Phys. Rev. Lett.* **1996**, 77, 3427.
- Vanmaekelbergh, D.; de Jongh, P. E.; *J. Phys. Chem. B* **1999**, 103, 747.
- Dlocik, L.; Ileperuma, O.; Lauermann, I.; Peter, L. M.; Ponomarev, E. A.; Redmond, G. *J. Phys. Chem. B* **1997**, 101, 10281.
- Franco, G.; Gehring, J.; Peter, L. M.; Ponomarev, E. A.; Uhlenendorf, I. *J. Phys. Chem. B* **1999**, 103, 692.
- (a) Fisher, A. C.; Peter, L. M.; Ponomarev, E. A.; Walker, A. B.; Wijayantha, K. G. U. *J. Phys. Chem. B* **2000**, 104, 949. (b) Peter, L. M.; Wijayantha, K. G. U. *Electrochem. Commun.* **1999**, 1, 576.
- Solbrand, A.; Lindström, H.; Rensmo, H.; Hagfeldt, A.; Lindquist, S.-E. *J. Phys. Chem. B* **1997**, 101, 2514.
- Solbrand, A.; Henningsson, A.; Södergren, S.; Lindström, H.; Hagfeldt, A.; Lindquist, S.-E. *J. Phys. Chem. B* **1999**, 103, 1078.
- Schwarzburg, K.; Willing, F. *J. Phys. Chem. B* **1999**, 103, 5743.
- Nelson, J. *Phys. Rev. B* **1999**, 59, 15374.
- van de Lagemaat, J.; Frank, A. J. *J. Phys. Chem. B* **2000**, 104, 4292.
- Schlichthörl, G.; Huang, S. Y.; Sprague, J.; Frank, A. J. *J. Phys. Chem. B* **1997**, 101, 8141.

- (16) Schlichthörl, G.; Park, N. G.; Frank, A. J. *J. Phys. Chem. B* **1999**, *103*, 782.
- (17) Kopidakis, N.; Schiff, E. A.; Park, N.-G.; van de Lagemaat, J.; Frank, A. J. *J. Phys. Chem. B* **2000**, *104*, 3930.
- (18) Nelson, J.; Haque, S. A.; Klug, R. D.; Durrant, J. R. *Phys. Rev. B* **2001**, *63*, 205321.
- (19) van de Lagemaat, J.; Frank, A. J. *J. Phys. Chem. B* **2001**, *105*, 11194.
- (20) Biswas, A. M.; Haque, S. A.; Lutz, T.; Montanari, I.; Olson, C.; Willis, R. L.; Durrant, J. R.; Nelson, J. *IEEE 28th Photovoltaic Specialist Conference, Conference Proceeding* **2000**, 796.
- (21) Wang, H.; He, J.; Boschloo, G.; Lindström, H.; Hagfeldt, A.; Lindquist, S.-E. *J. Phys. Chem. B* **2001**, *105*, 2529.
- (22) M. Späth, J. M. Kroon, P. M. Sommeling, J. A. Wienke, J. A. M. van Roosmalen, *26th IEEE Photovoltaic Specialist Conference, Conference Proceeding* **1997**, 503.
- (23) Pichot, F.; Pitts, R.; Gregg, B. A. *Langmuir* **2000**, *16*, 5625.
- (24) Lindström, H.; Holmberg, A.; Magnusson, E.; Lindquist, S.-E., Malmqvist, L.; Hagfeldt, A. *Nano Lett.* **2001**, *2*, 97.
- (25) Nakade, S.; Kambe, S.; Wada, Y.; Kitamura, T.; Yanagida, S. *IEEE 28th Photovoltaic Specialist Conference, Conference Proceeding* **2000**, 802.
- (26) Park, N.-G.; Schlichthörl, G.; van de Lagemaat, J.; Cheong, H. M.; Mascarenhas, A.; Frank, A. J. *J. Phys. Chem. B* **1999**, *103*, 3308.
- (27) Saito, Y.; Kambe, S.; Wada, Y.; Kitamura, T.; Yanagida, S. Manuscript submitted for publication.
- (28) Kambe, S.; Nakade, S.; Wada, Y.; Kitamura, T.; Yanagida, S. *J. Mater. Chem.* **2002**, *12*, 723.
- (29) In refs 10 and 11, a three electrode cell was used. When we set up the experiment, we used a three electrode setup and found that 0–+300 mV vs Ag/AgCl bias did not change the transient current peak time. Hence, we used a two electrode cell here. About electrolyte, we have seen changes of the transient peak time and amplitude, which might be caused by electrolyte decomposition after tens of measurements. To avoid the influence, the electrolyte was changed frequently, and the peak time was checked before and after the change.
- (30) Nakade, S.; Kambe, S.; Wada, Y.; Kitamura, T.; Yanagida, S. *J. Phys. Chem. B* **2001**, *105*, 9150.
- (31) Saturation of J_{sc} from P25_150 at thin films was also reported in ref 25.
- (32) van de Lagemaat, J.; Park, N.-G.; Frank, A. J. *J. Phys. Chem. B* **2000**, *104*, 2044.
- (33) Kambe, S.; Nakade, S.; Kitamura, T.; Wada, Y.; Yanagida, S. *J. Phys. Chem. B* **2002**, *106*, 2967.
- (34) The results on ref 25 indicated that the charge traps on the surface of P25 would not be removed by 450 °C annealing.
- (35) Duffy, N. W.; Peter, L. M.; Rajapakse, R. M. G.; Wijayantha, K. G. U. *Electrochem. Commun.* **2000**, *2*, 658.
- (36) On ref 25, it was reported that the electron lifetime of low-temperature annealed films are longer than that of high-temperature annealed films, based on the open circuit voltage decay measurements. This seems to contradict with the results on this paper. The measurements on the ref 25 were performed without dye in ethanol containing LiClO₄ by a UV laser pulse. The difference may come from the different electrolyte, the density of electrons in the film, and/or the dye adsorption.
- (37) Ferber, J.; Luther, J. *J. Phys. Chem. B* **2001**, *105*, 4895.
- (38) Shklover, V.; Ovchinnikov, Yu. E.; Braginsky, L. S.; Zakeeruddin, S. M.; Grätzel, M. *Chem. Mater.* **1998**, *10*, 2533.